Molecular Biology of the Cell
Vol. 19, 428–437, January 1, 2009

# Cells Lacking the Fragile X Mental Retardation Protein (FMRP) have Normal RISC Activity but Exhibit Altered Stress Granule Assembly

**Marie-Cécile Didiot, Murugan Subramanian, Eric Flatter, Jean-Louis Mandel, and Hervé Moine**

IGBMC (Institut de Génétique et de Biologie Moléculaire et Cellulaire); Inserm, U596; CNRS, UMR7104; and Université Louis Pasteur, Collège de France, Chaire de Génétique Humaine, Illkirch-Graffenstaden, F-67404 France

Submitted July 18, 2008; Revised October 22, 2008; Accepted October 30, 2008
Monitoring Editor: A. Gregory Matera

**The fragile X mental retardation protein (FMRP) is an RNA-binding protein involved in the mRNA metabolism. The absence of FMRP in neurons leads to alterations of the synaptic plasticity, probably as a result of translation regulation defects. The exact molecular mechanisms by which FMRP plays a role in translation regulation have remained elusive. The finding of an interaction between FMRP and the RNA interference silencing complex (RISC), a master of translation regulation, has suggested that both regulators could be functionally linked. We investigated here this link, and we show that FMRP exhibits little overlap both physically and functionally with the RISC machinery, excluding a direct impact of FMRP on RISC function. Our data indicate that FMRP and RISC are associated to distinct pools of mRNAs. FMRP, unlike RISC machinery, associates with the pool of mRNAs that eventually goes into stress granules upon cellular stress. Furthermore, we show that FMRP plays a positive role in this process as the lack of FMRP or a point mutant causing a severe fragile X alter stress granule formation. Our data support the proposal that FMRP plays a role in controlling the fate of mRNAs after translation arrest.**

## INTRODUCTION

Fragile X syndrome, the most common form of inherited mental retardation, is caused by the absence of the fragile X mental retardation protein (FMRP). FMRP is an RNA-binding protein involved in the posttranscriptional control of target mRNAs in particular at the level of synapses where the absence of its function could alter synaptic plasticity and the cognitive functions (Castets *et al.*, 2005; Garber *et al.*, 2006; Huber, 2006). FMRP was found to be associated specifically with distinct classes of mRNAs: mRNAs harboring G-quartet, poly (U) stretches, or a kissing complex motif (Schaeffer *et al.*, 2003; Jin *et al.*, 2004a; Darnell *et al.*, 2005). An indirect interaction of FMRP with several mRNAs has also been proposed through its interaction with the noncoding BC1 RNA (Zalfa *et al.*, 2003), but the biological importance of this later type of interaction appears unclear (Iacoangeli *et al.*, 2008). Generally FMRP was found associated with several aspects of the RNA metabolism, notably translation repression (Laggerbauer *et al.*, 2001; Castets *et al.*, 2005), transport (Dictenberg *et al.*, 2008), and degradation (Zalfa *et al.*, 2007). These cellular events are generally related to translation arrest. Several of the mRNAs targeted by FMRP are candidates for a translation repression (e.g., PP2A; Castets *et al.*, 2005) and MAP1B, Zhang *et al.*, 2001), but the molecular mechanism by which this repression occurs is still largely unknown. The finding of the interaction of FMRP, and its *Drosophila* ortholog dFXR, with the RNA Interference Silencing Complex (RISC; Caudy *et al.*, 2002; Ishizuka *et al.*, 2002; Jin *et al.*, 2004a,b) suggested that there could be a functional link between FMRP and the RISC. Thus, it was proposed that FMRP could be a modulator of the RISC function. Conversely, the RISC could have been an effector of the FMRP-mediated translational control or a combination of both (Schaeffer *et al.*, 2003). Up to now, however, a clear demonstration of a direct role of FMRP in the RNA interference (RNAi) and/or microRNA pathways controlled by the RISC has been lacking. In fact it was proposed that dFXR-deficient *Drosophila* S2 cells could have either no (Ishizuka *et al.*, 2002) or a moderate impact (Caudy *et al.*, 2002) on RNAi efficiency, and more recently FMRP was described to have a positive impact on small interfering RNA (siRNA) efficiency in mouse fibroblast cells (Plante *et al.*, 2006).

To answer the question of the relationship between FMRP and the RISC pathways and to examined the link between FMRP and silent mRNAs in general, we analyzed the localization of endogenous FMRP protein in cells with respect to two known cellular structures where nontranslated mRNAs have been shown to accumulate: the processing bodies (PBs) and the stress granules (SGs) where RNA silencing and integrated stress response are proposed to occur, respectively. We also examined several aspects of the potential physical and functional relationship between FMRP and the RISC machinery in cells. In our model systems, FMRP was found to have distinct localization properties than the component of the RISC machinery and to have no impact on RISC efficiency in various cell types. We identify however a

This article was published online ahead of print in *MBC in Press* (http://www.molbiolcell.org/cgi/doi/10.1091/mbc.E08–07–0737) on November 12, 2008.

Address correspondence to: Hervé Moine (moine@igbmc.u-strasbg.fr).



© 2008 by The American Society for Cell Biology

new role of FMRP in mRNA metabolism as an effector of stress granule assembly.

## MATERIALS AND METHODS

### Plasmids

pTL1-Iso7 and pTL1-Iso7-I304N encoding isoform 7 FMRP protein wild type and mutation I304N, respectively, were described previously (Sittler *et al.*, 1996; Castets *et al.*, 2005).

***pRLTK-1x.*** The insertion of one miRNA23 target in the 3′ untranslated region (UTR) of the *Renilla* luciferase (Rluc) gene in pRL-TK vector (Promega, Madison, WI) was performed with QuickChange site-directed mutagenesis kit (Stratagene, La Jolla, CA) using oligonucleotides sense 5′-CATGTCTGCTCGAAGCGGTCACTTTCCAGTGAGTTCCAGCCGCTCTAGAATTATTGT-3′ and antisense 5′-ACAATAATTCTAGAGCGGCTGGAACTCACTGGAAAGTGACCGCTTCGAGCAGACATG-3′ following the manufacturer's instructions.

***pRLTK-5x.*** The five target site-containing pRLTK was constructed with the two partially complementary DNA oligonucleotides: sense 5′-GCTCTAGATGGAACTCACTGGAAAGTGACATATCTGGAACTCACTGGAAAGTGACGAACTTGGAACTCACTGGAAAGTGACATGAC-3′ and antisense 5′-GCTCTAGAGTCACTTTCCAGTGAGTTCCAATATCGTCACTTTCCAGTGAGTTCCAGTCATGTCACTTTCCAGTGAGTTCCAAGTTC-3′. The two oligonucleotides were annealed 5 min at 95°C, filled with Taq DNA polymerase 10 min at 72°C, cut with XbaI, and ligated into 3′UTR of pRL-TK XbaI site.

***pRLTL5x-FBS.*** FBS sequence was produced by PCR using oligonucleotides.

The original BamHI site was remove from pRL-TK by PCR-directed mutagenesis using oligonucleotide 5′-GTGCCACCTGGATACTTATCGATTTTACC-3′. SalI and BamHI sites were added at the 3′ end of the five siRNA target sites by PCR-directed mutagenesis using oligonucleotide 5′-CCAAACTCATCAATGTATCTTATCATGTGGATCCACTGCAGTCGACCTGCTCGAAGCGGCCGCTCTAG-3′.

### Short Duplex RNA Preparation

The oligonucleotide-directed synthesis of small RNA transcripts was performed with T7 RNA polymerase as previously described (Donze and Picard, 2002). One nanomole of each DNA oligonucleotide (P-sense, 5′-TGGAACTCACTGGAAAGTGACTATAGTGAGTCGTATTA; P-antisense, 5′-AAGTCACTTTCCAGTGAGTTCTATAGTGAGTCGTATTA; B-sense 5′-TGGAACTCACACCAAAGTGACTATAGTGAGTCGTATTA; B-antisense, 5′-AAGTCACTTTGGTGTGAGTTCTATAGTGAGTCGTATTA) was annealed with 1 nmol of T7 oligonucleotide (5′-TAATACGACTCACTATAC) in 50 $\mu$l of Tris-EDTA buffer, pH 8.0, for 3 min at 95°C followed by slow cooling to 20°C. Transcriptions were performed in 50 $\mu$l of mix (1× T7 RNA polymerase buffer, 4 mM spermidine, 20 mM DTT, 0.1 mg/ml BSA, 4 mM each rNTP, 16 mM rGMP, 20 U RNAsin, and 5 U T7 RNA polymerase) on 400 pmol of annealed dsDNA template at 37°C for 2 h and treated with RNAse free DNAse. Sense and antisense 21-nt RNAs were then purified on 8 M urea, 25% polyacrylamide gel run at 30 mA in a Tris-borate-EDTA buffer. RNAs were visualized by UV shadowing, excised, and eluted in 200 $\mu$l of 0.5 M $NH_4$acetate, 0.1 mM EDTA for 12 h at 4°C. RNAs were ethanol-precipitated and resuspended in water. Perfect and bulged sdRNAs were generated by mixing 1 nmol of each purified sense and antisense 21-nt RNA at 95°C for 5 min and for 1 h at 37°C.

### Mouse Embryonic Fibroblasts Preparation

Pregnant female mice were killed by cervical dislocation at day 13 after coitus, and embryos were harvested. The head and the dark red organs were cut away from each embryo. Embryos were minced in 500 $\mu$l phosphate-buffered saline (PBS) and passed through an 18-gauge needle. Suspended cells were plated in 60-mm dishes in 2 ml of Dulbecco's modified Eagle's medium (DMEM) supplemented with 15% fetal calf serum and antibiotics at 37°C, 5% $CO_2$. After 2 d, mouse embryonic fibroblasts (MEFs) were grown in DMEM supplemented with 10% fetal calf serum and 1 g/l glucose in the presence of antibiotics at 37°C in 5% $CO_2$.

### Cell Culture and Transfections

HeLa cells and all adherent mouse fibroblasts were grown in DMEM supplemented with 10% fetal calf serum, 1 g/l glucose in the presence of antibiotics at 37°C in 5% $CO_2$. Four hours before transfection, $4 \times 10^4$ cells were plated into 24-well format plates in 500 $\mu$l of antibiotic-free medium. Transfections were performed in triplicate with Lipofectamine 2000 (Invitrogen, Carlsbad, CA) as directed by the manufacturer with 300 ng of pTL1-Iso7 or pTL1-Iso7-I304N. Twenty-four hours later, 100 ng of the reporter gene (pRLTK, pRLTK-1x, or pRLTK-5x, pRLTK-5x-FBS) were cotransfected by using Lipofectamine 2000 with 100 ng of the pFlashSV40 plasmid (Synapsys Solutions, Burgess Hill, West Sussex, United Kingdom), coding for the *Firefly* luciferase (Fluc) and used as normalizer, and 1–20 nM of sdRNA in a final volume of 600 $\mu$l for each well. A nonspecific sdRNA scramble from Dharmacon Research (Boulder, CO; D-001205-01-05) was used as negative control at 5 nM. Plasmid pEGFP-hAgo2 expressing fusion GFP-human Ago2/eIF2C2 (W. Filipowicz, FMI, Basel, Switzerland) was transfected in HeLa cells in a 24-well format, using 0.8 $\mu$g DNA with Lipofectamine 2000 following the manufacturer's instructions.

### Luciferase Assays

Rluc and Fluc activities were determined using Luciferase Assay System (Promega) according to the manufacturer's protocol. Assays were performed 24 h after transfection. Cell monolayers in 24-well cluster dishes were removed by scraping into 100 $\mu$l of reporter lysis buffer. Luciferase activities were measured using a Lumat LB 9501 luminometer (Berthold, Pforzheim, Germany). Rluc values were normalized with Fluc control values.

### Real-Time Reverse Transcriptase PCR

To evaluate the expression of *Renilla* and *Firefly* mRNAs, total RNAs were extracted from transfected cells by using GenElute Mammalian Total RNA kit

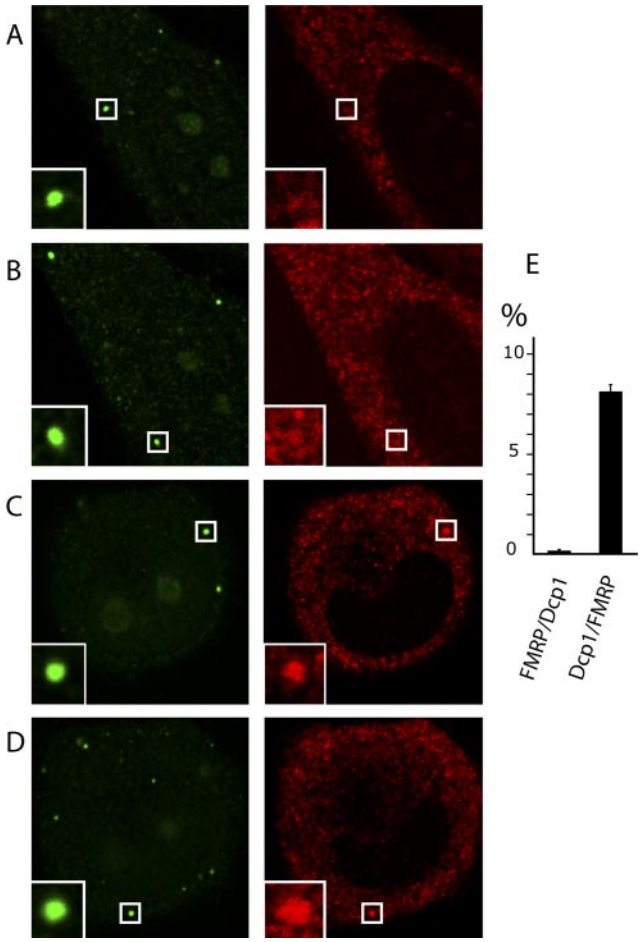



**Figure 1.** The majority of FMRP is not present in PBs in HeLa cells. Confocal microscopy analysis of FMRP (red) and Dcp1 (green) densities. Endogenous FMRP was stained with anti-FMRP antibody (1C3) and an Alexa-fluor 594–labeled anti-mouse secondary antibody. Endogenous Dcp1 was stained with an anti-Dcp1a antibody and an Alexa-fluor 488–labeled anti-rabbit secondary antibody. (A and B) Two different stacks taken 2 $\mu$m apart from of one representative cell. (C and D) Two stacks from a cell showing a weak colocalization of FMRP with PBs. These cells represent <10% of cell population. (E) Graph summarizing the colocalization of FMRP and Dcp1 in HeLa cells. FMRP/Dcp1, indicates the percentage of FMRP densities colocalizing with the Dcp1 densities (0.05 ± 0.02%). Dcp1/FMRP, indicates the same for Dcp1 densities colocalizing with the FMRP densities (8 ± 0.8%). The data are averages of 15 Z stacks from 10 different representative cells (see *Materials and Methods*). Error bars, SDs.

(Sigma, L'isle d'Abeau, France) as described by the manufacturer's protocol. Reverse transcription reactions were performed on 0.5 $\mu$g of total RNA by using SuperScript III Reverse Transcriptase kit (Invitrogen) as described by the manufacturer. Real-time PCR was performed on 1:100 dilution of each reverse transcription sample in triplicate by using Platinum SybrGreen qPCR SuperMix (Invitrogen) in the MX4000 Thermocycler (Stratagene; 40 PCR cycles, denaturation at 95°C for 15 s, annealing at 55°C for 30 s, and extension at 72°C for 30 s). The real-time PCR reactions were carried out in the presence of 10 pmol of *Renilla* (forward 5′-TCTTCGTGGAAACCATGTTG-3′; reverse 5′-TGTTGGACGACGAACTTCAC-3′) and *Firefly* (forward 5′-TTCCATCT-TCCAGGGATACG-3′; reverse 5′-ATCCAGATCCACAACCTTCG-3′) gene-specific primers. The fluorescence was monitored at each annealing step. The *Firefly* reporter gene served as an internal control to monitor the transfection efficiency.

### *Polysomes Preparation*

HeLa cells washed twice in PBS were lysed directly in the 10-cm plates in a lysis buffer containing 50 mM Tris-HCl, 100 mM KCl, 5 mM $MgCl_2$, 1 mM DTT, 100 $\mu$g/ml cycloheximide, 40 U/ml RNasin (Sigma), Mini Complete antiprotease EDTA free (Roche, Indianapolis, IN) and 1% NP-40 or 1% sodium deoxycholate as indicated in text. Total mouse embryonic day 16 (E16) brains were homogenized in 700 $\mu$l of lysis buffer without detergent by hand in a Kontes glass homogenizer (Vineland Glass Co., Vineland, NJ) fitted with the loose-B pestle. The samples were transferred in microtubes, and 1% NP-40 was added to lyse the cells. The samples were centrifuged at 13,000 rpm at 4°C for 10 min. For fractionation, the clarified lysates were loaded on 15–45% sucrose gradients and separated by ultracentrifugation with a SW41 rotor (Beckman) at 36,000 rpm at 4°C for 2 h. Linear sucrose gradients (15–45%) were prepared with a Master Gradient 107ip (BioComp Instruments, Fredericton, NB, Canada) as indicated by the manufacturer in polyallomer tubes (Beckman Instruments, Fullerton, CA). Fractions of 500 $\mu$l were collected and $A_{260}$ was measured using a continuous flow cell UV detector (GE Healthcare Life Sciences, Piscataway, NJ). Polysomes of each fractions were precipitated with 2.5 vol of 100% ethanol with an incubation at −20°C overnight and by centrifugation at 13,000 rpm at 4°C for 20 min. Pellets were washed in 70% ethanol, briefly dried, and resuspended directly in SDS loading buffer.

### *Western Blotting*

After denaturation in the loading buffer (100 mM Tris-HCl, pH 6.8, 4% SDS, 30% glycerol, 1.4 M $\beta$-mercaptoethanol, and bromophenol blue) for 3 min at 95°C, proteins present in each polysome fraction were analyzed on a 6% SDS-polyacrylamide gel and immunoblotted onto nylon membrane (Schleicher & Schuell, Keene, NH) in Tris-glycine-SDS/20% ethanol buffer for 1 h at 200 mA. Membranes were incubated overnight at 4°C with mouse anti-FMRP 1C3 1:1000 (Devys *et al.*, 1993), rabbit anti-hAgo2/GERp95 1:500 (Cikaluk *et al.*, 1999), mouse anti-eIF2C2 1:1000 (ab57113, Abcam, Cambridge, MA), and

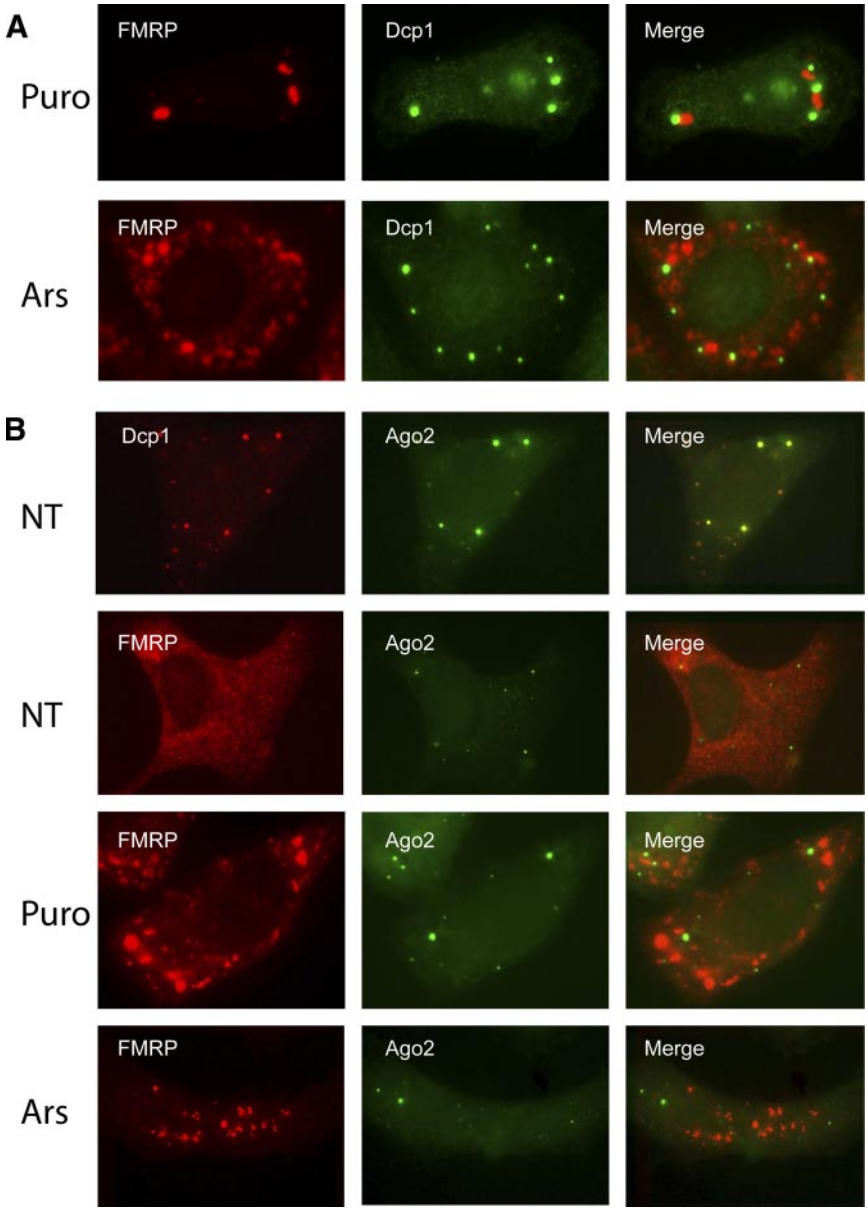



**Figure 2.** FMRP and Ago2 are localized in distinct subcellular compartments after various cellular stresses in HeLa cells. (A) FMRP is segregated in close but distinct subcellular compartments than Dcp1 when translation was arrested with 2 mM puromycin for 1 h (Puro) or 500 $\mu$M arsenite for 30 min (Ars). Immunolabeling was as described in Figure 1. (B) Ago2 (GFP-hAgo2 transiently transfected) is localized in PBs like Dcp1 in nontreated cells (NT) and remains there, unlike FMRP (immunolabeled as in Figure 1), after 2 mM puromycin for 1 h (Puro) or 500 $\mu$M arsenite for 30 min (Ars). The selected cells are representative of the majority of cells expressing low or moderate level of GFP-hAgo2.

anti-ribosomal protein L7 antisera (Ziemiecki *et al.*, 1990) and then incubated at room temperature with peroxidase-conjugated goat anti-rabbit or goat anti-mouse antibodies (1/5000). Immunoreactive bands were visualized with the SuperSignal West Pico Chemiluminescent Substrate (Pierce, Rockford, IL).

### *Immunofluorescence and Fluorescent In Situ Hybridization*

Cells for immunofluorescence (IF) and fluorescent in situ hybridization (FISH) were grown on glass coverslips, coating with poly-D-lysine, and addition of fibronectin (1 pg/ml) was used for lymphoblast cultures. Cultures were incubated at 37°C in 5% $CO_2$. Stress treatments were performed by incubating the cells at 43°C or with sodium arsenite (500 $\mu$M final) for indicated time. After two washes with PBS, cells were fixed with PBS/4% paraformaldehyde (pH 7) at room temperature for 20 min. Cells were then washed for 15 min with 50 mM $NH_4Cl$ and permeabilized with PBS/0.2% Triton-X for 10 min at room temperature. Cells for IF were washed with PBS and blocked for 1 h at room temperature in PBS/0.1% Triton-X containing 5% BSA. Cells were incubated with primary antibodies mouse anti-FMRP 1C3 1:1000, rabbit anti-hDcp1a 1:1000 (J. Lykke-Andersen, University of Colorado), goat anti-TIA-1 1:1000 (C-20, Santa Cruz Biotechnology, Santa Cruz, CA), rabbit anti-MLN51 1:1000 (C. Tomasetto, IGBMC, Illkirch, France) or rabbit anti-eIF4E (FL-217, tebu-bio Laboratories, Le Perray-en-Yvelines, France), 1:1000 diluted in PBS/0,1% Triton-X overnight at 4°C. After three washes in PBS/0.1% Triton-X, cells were incubated with indicated fluorescent secondary antibodies (1:500) for 1 h at room temperature. Cells were washed three times at room temperature in PBS/0.1% Triton-X for 10 min and mounted in a Vectashield Mounting Medium with DAPI (1.5 $\mu$g/ml; Vector Laboratories, Burlingame, CA). Cells for FISH were rehydrated with 2× SSC/50% formamide during 5 min at room temperature and then hybridized with 20 ng of oligo-dT probe in hybridization solution (2× SSC, 50% formamide, 30 $\mu$g *E. coli* tRNA, 0.02% RNAse-free BSA, 2 mM vanadyl-ribonucleoside complexes, and 10% sulfate dextran) 12 h at 37°C in 40 $\mu$l. Oligo-dT probe was first heated 1 min at 90°C in 2× SSC/50% formamide and tRNA. Cells were washed two times at room temperature in 2× SSC/50% formamide for 20 min and mounted as above. All image acquisitions and quantification of fluorescent signal intensities were performed using standardized settings on a microscope (model DM4000 B, Leica, Deerfield, IL) equipped with CCD camera (CoolSnap CF, color) with 40× or 63× objectives and a confocal microscope (model SP1 and SP2-MP, Leica) with a 100× objective. For colocalization analyses, JACoP localization analysis tool with ImageJ (http://rsb.info.nih.gov/ij/) was used on confocal images to determine Manders overlap coefficient (Bolte and Cordelieres, 2006). For SG quantification analysis, randomly selected images from each experiment were analyzed by counting SGs in at least 100 cells.

## RESULTS

### *FMRP Localizes to Cytoplasmic Granules and SGs and Has Little Overlap with PBs*

We first compared by immunofluorescence the localization of FMRP with the PB marker protein Dcp1a, which localizes as bright foci punctuating the cytoplasm of nearly all cells. In HeLa cells, FMRP was found distributed throughout the cytoplasm in a granular manner with no overlap with PBs (Figure 1, A and B). Occasionally, (i.e., in <10% of the cells), some FMRP granules were found to colocalize with PBs (Figure 1, C and D). Applying JACoP localization analysis tool with ImageJ (Bolte and Cordelieres, 2006) on confocal stacks, the percentage of FMRP signal that overlapped with PBs was estimated to be 0.05 ± 0.02% (Figure 1E). A similar value was found when the fluorophores of the secondary antibodies were inverted (data not shown). Thus, FMRP was essentially excluded from PBs. This indicated that FMRP and Dcp1 are present in distinct subcellular compartments and only a very small fraction of total FMRP could potentially colocalize with PBs. The round shape of cells showing a partial colocalization of FMRP and PBs may indicate they are in mitotic phase. These data suggest that if FMRP is interacting with members of the RISC complex as previously proposed, this interaction concerns only a very minor fraction of FMRP pool and/or occurs in a narrow time frame. Furthermore, this interaction should cease before the mRNAs submitted to RISC accumulate in PBs.

FMRP has been shown to be a component of SGs (Mazroui *et al.*, 2002), and PBs and SGs have been shown to be two types of RNA granule structures in close relationship with each other (Kedersha *et al.*, 2005). We then examined the relationship between FMRP, PBs, and SGs. We followed the behavior of FMRP after different treatments that induce the release of mRNAs from polyribosomes or their stabilization and differently affect SGs and PBs. It has been shown previously that puromycin, an aminoacyl-tRNA analog that causes translation blocking by polysomes disassembly with premature release of polypeptide chain and mRNA, leads to an increase of the size and number of PBs (Sheth and Parker, 2003; Kedersha *et al.*, 2005; Anderson and Kedersha, 2006). After puromycin treatment, FMRP was found localized in a few large granules close but distinct from PBs (Figure 2A). It was previously shown that such treatment leads to SGs assembly (Kedersha *et al.*, 2000) as well as to PBs enlargement (Eulalio *et al.*, 2007). Thus, when mRNAs are released from polysomes by puromycin, FMRP localizes in SGs. Arsenite treatment had similar effect as puromycin (Figure 2B). After 30 min of 500 $\mu$M arsenite treatment or 15 min at 43°C (see Figure 5, B and C, respectively), all immunodetectable FMRP appeared in SGs as defined by the SG marker TIA-1. Meanwhile, the PBs remained unaffected or slightly increased in size. We showed next that this behavior is clearly distinct from that of the core protein of the RISC, Ago2. In nontreated cells Ago2 is localized in PBs like Dcp1 (Figure 2B, NT). On arsenite and puromycin treatment, Ago2 remained in PBs (Figure 2B) unlike FMRP that assembled into SGs. Thus, FMRP, by being segregated away from the PBs in conditions where the RISC members were found to accumulate (Pillai *et al.*, 2005; Eulalio *et al.*, 2007), exhibit a clear distinct cellular behavior than the RISC components. Cycloheximide treatment, which blocks translation at the elonga-

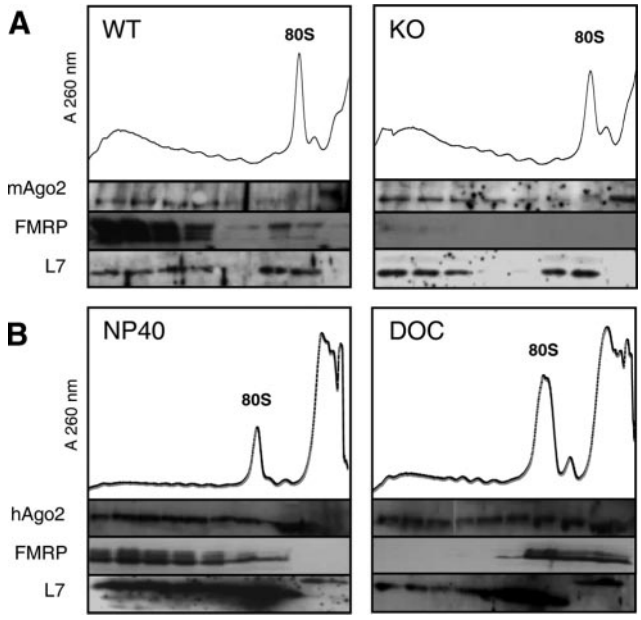



**Figure 3.** Fractionation of Ago2 and FMRP on sucrose gradients. (A) Comparison of FMRP and mAgo2 mobility in 15–45% sucrose gradient prepared from wild-type or knockout littermate embryonic mouse brain extracts. The densitograms ($A^{260}$) of gradients are shown with corresponding pooled fractions tested for FMRP, ribosomal protein L7, and mAgo2 by Western blot analysis. (B) Comparison of FMRP and hAgo2 mobility in 15–45% sucrose gradient prepared with HeLa cell extracts submitted to NP-40 or sodium deoxycholate (DOC) detergeants. The densitograms ($A^{260}$) are shown with fractions tested for FMRP, ribosomal protein L7, and hAgo2 by Western blot analysis.

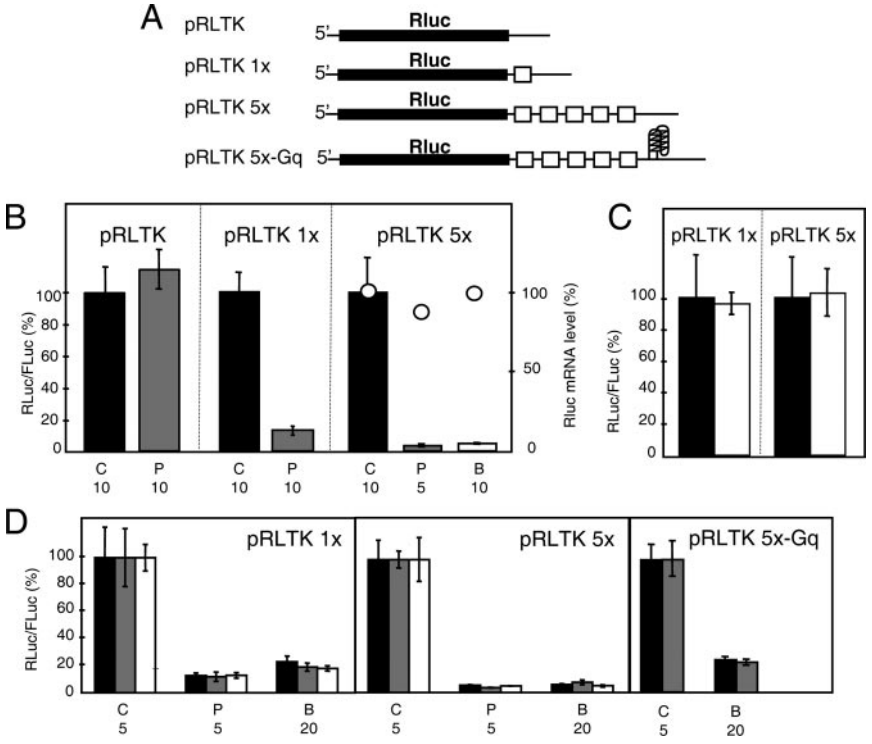



**Figure 4.** FMRP has no impact on RISC activity. (A) Scheme of the reporter gene *Renilla luciferase* mRNAs (Rluc) bearing no (pRLTK), one (pRLTK1x), five targets (pRLTK5x) of miR23/short duplex RNAs (sdRNA), or one target combined with a FMRP binding site (pRLTK5x-Gq). (B) Controls of the RISC activity assay. On the various *Rluc* mRNA constructs in HeLa cells extracts. C (■), P (▨), and B (□) are small duplex RNAs with no complementarity and perfect and imperfect matches with *Rluc* mRNA, respectively. The concentrations of small duplex RNAs (5 or 10 nM) used to treat cells are given below the graph. The ratio of Rluc to Fluc activities (Rluc/Fluc) set to 100 for the control is given. The relative amount of *Rluc-5X* mRNA reporter (as determined by real-time reverse transcriptase PCR) is indicated (○) with the different sdRNAs. (C) Influence of FMRP on endogenous miR23 activity. Normalized Rluc activities of reporters bearing one (pRLTL1x) or five targets (pRLTK5x) transfected in FMRP wild-type (■) and knockout (□) MEF extracts are shown. (D) Influence of FMRP on sdRNA-dependent RISC activity. Rluc/Fluc values measured in mouse *FMR1*$^{-/-}$ fibroblasts (Mazroui *et al.*, 2002) transfected with empty vector as control (■) or transfected with pTL1-Iso7 expressing wild-type FMRP major isoform 7 (▨) or pTL1-Iso7-I304N expressing mutant I304N FMRP isoform 7 (□). C, P, and B are small duplex RNAs with no complementarity and perfect and imperfect matches with *Rluc* mRNA, respectively. The concentrations of small duplex RNAs (5 or 20 nM) used to treat cells are given below the graph. The values in B, C and D are averages from at least three independent transfections performed in triplicate. Error bars, ± SD.

tion level without disrupting polyribosomes, induced instead both the granular distribution of FMRP to being more disperse and PBs to decline (data not shown).

These data suggest that FMRP and RISC are associated to distinct pools of mRNAs.

### *FMRP Exhibits Different Biochemical Behavior than Ago2 and Has No Impact on PBs Formation and RISC Activity*

The apparent discrepancy between the previously reported association of FMRP with members of the RISC complex, namely Ago2 (argonaute 2 or eIF2C2), and the here above reported differences in cellular localization, prompted us to examine further the relationship between FMRP and RISC. We first tested the possible impact of the absence of FMRP in cells on PBs formation. For this, we analyzed the number and intensity of PBs in MEFs from FMRP wild-type or knockout (*FMR1*$^{-/-}$) littermates. In these cells, no significant difference was observed either in PBs number or intensity as labeled with an anti-Dcp1 antibody (data not shown). Thus, the absence of FMRP has no impact on PBs formation in MEFs.

We then analyzed the influence of FMRP on the localization of Ago2, core of the RISC, in polyribosomes containing fractions of embryonic (E18) mouse brain extracts. Using Western blot analysis, Ago2 showed a ubiquitous localization throughout the sucrose density gradient, whereas FMRP was mostly concentrated in the heavy polyribosomes fractions (Figure 3A). In the polyribosomes prepared from littermate knockout mouse brain extracts, Ago2 had the same sedimentation profile, indicating that the absence of FMRP in cells had no detectable impact on Ago2 association to mRNAs. Because FMRP sedimentation behavior on sucrose density gradient is known to be sensitive to cationic detergent (Khandjian *et al.*, 2004), we then compared the behavior of Ago2 and FMRP with respect to the type of detergent used to extract polyribosomes. With the nonionic detergent NP-40, FMRP was found enriched in the heavy polyribosomes extracts of HeLa cells, whereas with the cationic sodium deoxycholate, FMRP was displaced from heavy particles to the 80S fraction (Figure 3B) as already reported (Khandjian *et al.*, 2004). Interestingly, Ago2 was insensitive to the nature of the detergent used. This indicated that FMRP and Ago2 had distinct mRNA interaction properties and likely belonged to different mRNP core complexes. The fact that a treatment of cells with puromycin induces the release of FMRP from heavy polysomes to free mRNPs (Stefani *et al.*, 2004), whereas the RISC members remain associated to polyribosomes-like migrating particles (Thermann and Hentze, 2007) further supports this idea.

We then tested the impact of FMRP on RISC activity using an Rluc reporter gene bearing in its 3′ UTR one or five targets of a microRNA (Figure 4A) as previously done to evidence the miRNA-dependent RISC activity in cell cultures (Doench *et al.*, 2003; Zeng *et al.*, 2003). The miRNA miR23 was chosen based on evidence for a role in neural specification (Kawasaki and Taira, 2003). The Rluc reporter gene borne on a plasmid was transfected in various cell lines together with a plasmid expressing the Fluc gene for normalization purpose. First, we validated the system by using short duplex RNAs (sdRNAs) that have been demonstrated to work as miRNAs or siRNAs, depending upon their complementarity with the target (Doench *et al.*, 2003; Zeng *et al.*, 2003). We tested both perfect (sdRNA P) and imperfect/bulged (sdRNA B) sdRNAs to mimic the siRNA or the miRNA pathways, respectively. In HeLa cells, when no target was present on the reporter gene or when a nonspe-

cific sdRNA (sdRNA C) was used, no effect was observed (Figure 4B, pRLTK). When one or five targets of the sdRNA was present in the 3′ UTR of the reporter gene, a specific and very efficient inhibition was seen that reached more than 90% with 10 nM of sdRNA B and 5 nM of sdRNA P (Figure 4B, pRLTK 1X and pRLTK 5X, respectively), this without apparent change in mRNA levels as measured by qRT-PCR with pRLTK 5X. This indicates that the inhibitory effect of both sdRNA P and B was at the translational level. Having validated our reporter constructions, we then assessed the action of endogenous miR23 in FMRP wild-type or FMRP-deficient MEFs. Although miR23 could be detected in these cells (Supplemental Figure S1), no impact of the FMRP absence on Rluc activity was detected whether one or five miR23 targets were present in Rluc mRNA (Figure 4C). To further trigger the siRNA or the miRNA pathways, we then performed the same experiments with the different small RNA duplexes described above. The efficiency of the sdRNAs P and B in FMRP knockout fibroblasts was very similar to the results obtained in HeLa cells (Figure 4D, ■). When FMRP major isoform 7 was expressed in these cells, the efficiency of the RISC activity was unchanged (Figure 4D, ▨). The same results were found independently of the complementarity of sdRNAs for its target (P or B), the number of targets in Rluc mRNA (pRLTK 1X or 5X), and the dose of sdRNAs (data not shown). The use of the loss-of-function mutant FMRP bearing the point mutation I304N in the second KH domain identified in a severe fragile X patient (De Boulle *et al.*, 1993) did not affect either these efficiencies (Figure 4D, □). Finally, we tested the contribution of an FMRP-binding site located nearby the sdRNA sites. When the guanine quartet RNA motif FBS previously demonstrated to bind FMRP in vitro (Schaeffer *et al.*, 2001) and in vivo (Rackham and Brown, 2004) was inserted 29 nucleotides downstream of the five miR23 targets, again, no specific effect was detected (Figure 4D, pRLTK5x-Gq). Altogether, these results indicate that the efficiency of the RISC activity does not rely on the presence of FMRP in cells.

### *Absence of FMRP or a Mutation in Its Second KH Domain Alters SGs Formation after Various Stresses*

We then compared the assembly of FMRP into SGs with other RNA-binding proteins known to localize in SGs, such as TIA-1, a splicing factor proposed to be a core component of SGs (Kedersha *et al.*, 1999), eIF4E, the Cap-binding protein of the initiation complex (Kedersha *et al.*, 2005) and MLN51, core protein of the exon junction complex (Baguet *et al.*, 2007). As expected, all four proteins that did not colocalize in normal conditions (Figure 5A) steadily and similarly localized into the SGs after a cellular stress such as arsenite treatment (Figure 5B). Unexpectedly, however, we noticed that these proteins had a different behavior after heat shock. Thus, although FMRP fully colocalized with TIA-1 after 15 min at 43°C, eIF4E was in majority located in different foci and MLN51 was absent from SGs (Figure 5C). These data suggest that heat shock triggers a different stress response than arsenite and that these mRNA-binding proteins have distinct functions and/or associate with distinct pools of mRNAs. Also, FMRP, like TIA-1, seemed to be an early SG assembly protein. As TIA-1 had been demonstrated to be a protein essential for SG formation (Kedersha *et al.*, 1999), we tested the possible involvement of FMRP in SGs formation.

We analyzed the ability of immortalized fibroblasts from FMRP knockout mice to form SGs, whether they had been stably transfected or not with the most frequent FMRP isoform 7 (Figure 6, A and B). Although the cells expressing FMRP very efficiently formed SGs, as visualized by immunofluorescence using anti-TIA-1 antibody and after oxidative stress or heat shock, cells lacking FMRP comparatively showed reduced SG formation. This reduction mostly affected the intensity rather than the number of SGs per cell. Interestingly, SG formation was also similarly impaired in cells stably expressing FMRP I304N (Figure 6A). Mutation I304N caused a stronger impairment on SG formation than

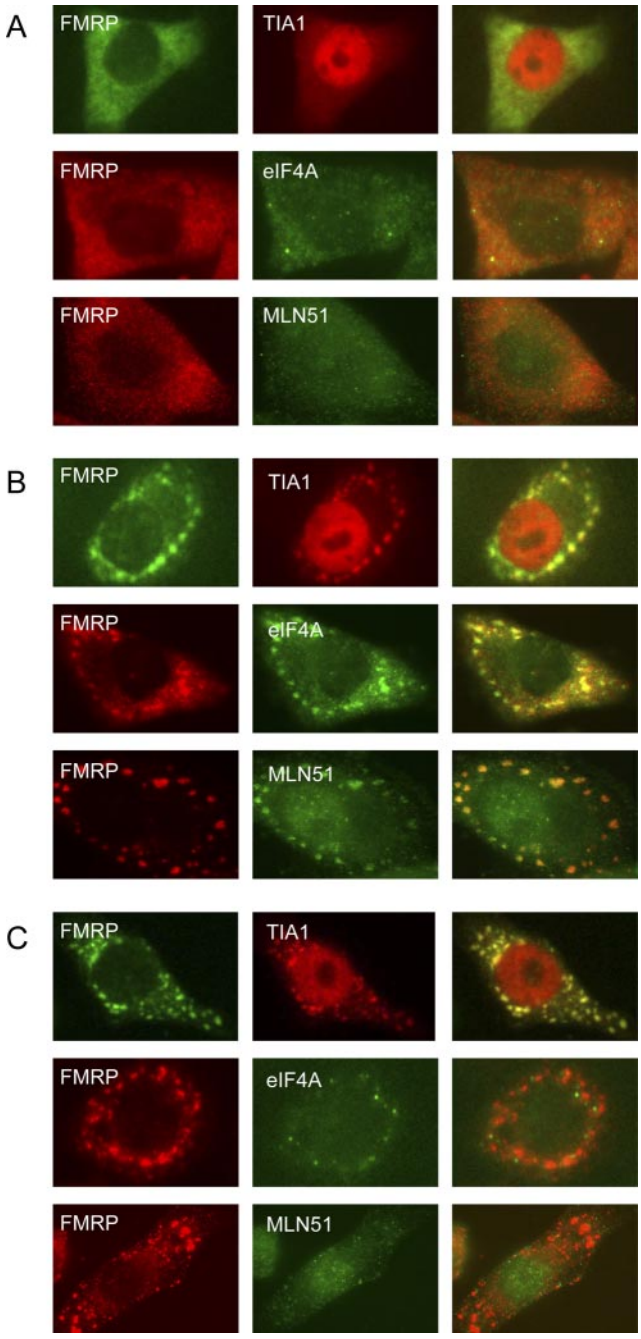



**Figure 5.** FMRP assembly in SGs. Fixed HeLa cells stained with an anti-FMRP antibody and anti-mouse secondary antibody labeled with Alexa-fluor 488 (green) or Alexa-fluor 594 (red), the anti-TIA-1 and anti-rabbit secondary antibody labeled with Alexa-fluor 594 (red), anti-eIF4E or anti-MLN51 and anti-rabbit secondary antibody labeled with Alexa-fluor 488 (green), in the following conditions: (A) nonstressed, (B) 500 $\mu$M sodium arsenite for 30 min, (C) 15 min at 43°C and with an anti-Dcp1a antibody.

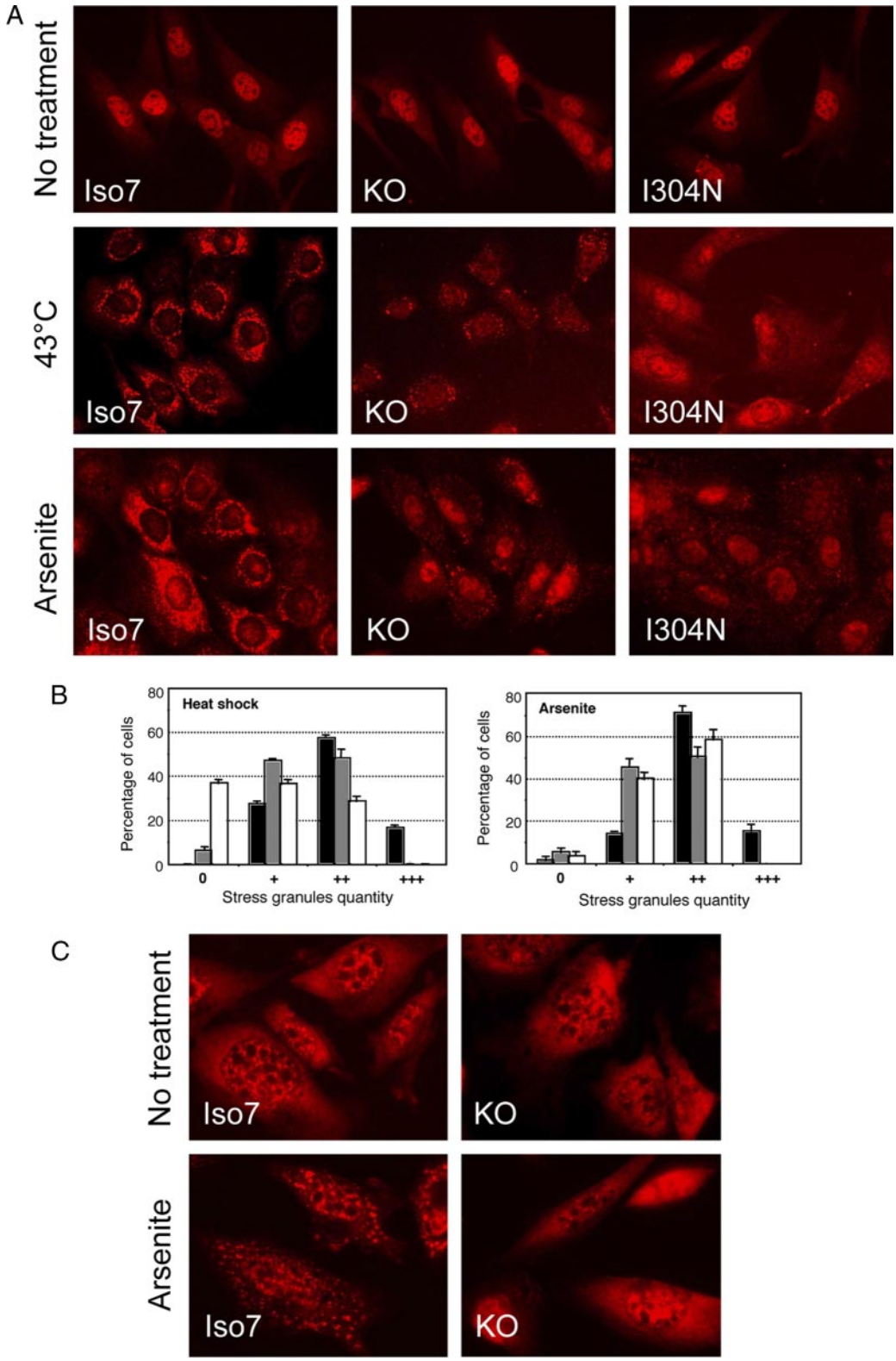



**Figure 6.** Absence of FMRP or point mutation I304N in its second KH domain impairs SG formation in mouse fibroblasts after various stresses. (A) SGs were visualized by immunocytofluorescence using an anti-TIA-1 antibody and anti-rabbit secondary antibody labeled with Alexa-fluor 594 (red) in fixed FMRP knockout fibroblasts stably transfected or not with FMRP isoform 7 (Iso7) or FMRP-I304N isoform 7 (I304N; Mazroui *et al.,* 2002). The nature of treatment is indicated for the various clones tested. (B) Histograms represent the percentages of cells (Y axis) for SGs quantity distributed in four categories: no granules (0), weak (+), moderate (++), and strong (+++) in wild-type (■), knockout (▨) and FMRP-I304N (□) cells. Experiments shown reflect at least three independent experiments with counting more than 100 cells in each case. (C) Fluorescent in situ hybridization with a poly-dT-Cy3 probe in fixed wild-type or knockout fibroblasts.

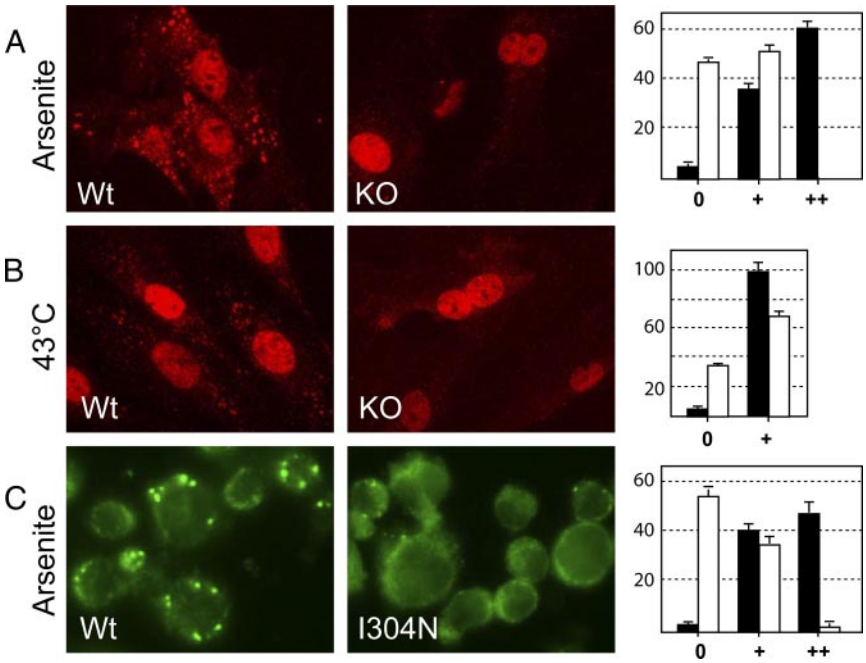



**Figure 7.** The lack of FMRP or the FMRP-I304N mutation results in SG assembly defects in various cells. (A) Arsenite induced SGs in MEFs from wild-type or knockout littermates, visualized with an anti-TIA-1 antibody and anti-rabbit secondary antibody labeled with Alexa-fluor 594 (red). (B) Heat-shock–induced SGs visualized as in A. (C) Arsenite induced SGs in human lymphoblasts from control individual (wild type) or from a fragile-X patient bearing the I304N mutation visualized with an anti-FMRP antibody and anti-rabbit secondary antibody labeled with Alexa-fluor 488 (green). Histograms represent the percentages of cells (Y axis) for SGs quantity distributed in two or three categories: no granules (0), weak (+), and moderate (++) in wild-type (■) and knockout or FMRP-I304N (□) cells.

the complete lack of FMRP after heat-shock treatment. SGs are proposed sites of mRNA storage during stresses. Defect in mRNA accumulation in SGs was visualized by using fluorescent in situ hybridization with a poly(A)-specific DNA probe (Figure 6C). Thus, mRNA storage in SGs after a cellular stress was affected in cells lacking FMRP. To exclude the possible influence of a clonal or immortalization effect on the cell physiology, we analyzed the SG formation in primary cultures of MEFs from wild-type or knockout littermates. A similar or stronger difference was observed between the wild-type and the knockout MEFs, with the knockout cells showing SG assembly defect both at intensity and number of SGs induced by oxidative stress (Figure 7A) and heat shock (Figure 7B), confirming the results observed in the immortalized cells. We then analyzed SG formation in a lymphoblastoid cell line from a patient expressing an FMRP protein bearing a point mutation I304N (De Boulle *et al.,* 1993). We compared the behavior of this cell line submitted to stress with the one from normal individuals (Figure 7C). Again, a marked defect in SG formation in response to stress was observed with the cells expressing the mutant FMRP protein in comparison with normal individuals. Altogether these data provide strong evidence that the absence of FMRP affects SG formation efficiency.

## DISCUSSION

In this study, we examined the relationship between FMRP, the protein absent in the fragile X syndrome, and two types of cytoplasmic granules: the PBs and the SGs where silent mRNAs are localized. PBs, also referred to as GW or Dcp bodies, are site where decapping and mRNA decay occur (Sheth and Parker, 2003; Cougot *et al.,* 2004). Recently, it was shown that mRNAs submitted to the RISC also accumulated in PBs (Liu *et al.,* 2005; Pillai *et al.,* 2005). SGs are foci where most mRNAs accumulate when cells are submitted to a stress and when general translation is arrested (Anderson and Kedersha, 2006). Both PB and SG RNA granules share many components and establish constant dynamic interactions (Anderson and Kedersha, 2002). We showed here that FMRP does not colocalize with PBs in HeLa cells as only 0.05% of immunoreactive FMRP colocalized with PBs. This quasi-absence of localization of FMRP within PBs contradicts the previously reported association of FMRP into the RISC seen in *Drosophila* (Caudy *et al.,* 2002; Ishizuka *et al.,* 2002) and HeLa cells (Jin *et al.,* 2004b). These results contradict also the previously reported colocalization of dFMRP within PBs in *Drosophila* neurons (Barbee *et al.,* 2006).

The absence of FMRP in cells has also no impact on PB formation contrarily to Ago2 and Dicer-2, which are required for PB integrity (Eulalio *et al.,* 2007). The absence of FMRP did not affect either the sedimentation profile of Ago2 on sucrose density gradient with mouse brain extracts, indicating that the association of Ago2 RISC to mRNAs was independent of FMRP. This together with the fact that the absence of FMRP has no impact on the RISC activity in immortalized or primary fibroblasts clearly indicates that FMRP is not a regulatory element of the RISC nor of PB related mRNA metabolism. Furthermore, FMRP and Ago2 have distinct behavior on sucrose density gradient: 1) the use of cationic detergent releases FMRP from heavy sedimenting particles, whereas Ago2 remains unchanged (this work) and 2) the puromycin treatment releases FMRP from polyribosomes (Stefani *et al.,* 2004), whereas mRNAs submitted to action of miRNAs (miRNPs) still migrates like "pseudopolysomes" (Thermann and Hentze, 2007). Altogether, these data suggest that FMRP and Ago2 belong to distinct complexes. This is further suggested by the fact that puromycin treatment, which releases mRNAs from translation pool, leads to accumulation of the RISC-silenced mRNAs into PBs (Sheth and Parker, 2003; Eulalio *et al.,* 2007), whereas it causes the segregation of FMRP (and some mRNAs) into the SGs. Thus, FMRP and Ago2 are likely associated with distinct pools of mRNAs.

The processes controlling the fate of an mRNA submitted to the RISC are still not well understood. In particular, it is not clear what causes a specific mRNA to be degraded or translationally repressed independently of its complemen-

tarity to a miRNA (Nilsen, 2007); for instance, in our hands both perfect and nonperfect sdRNA caused translation repression. As it was shown previously that FMRP has intrinsic RNA-binding properties, in particular for G-quartet RNA motifs (Darnell *et al.*, 2001; Schaeffer *et al.*, 2001), a possibility remained that FMRP could modulate the "susceptibility" of an mRNA to the RISC when already bound to this mRNA, for instance, through its nucleic acid chaperone properties that could enhance miRNAs hybridization (Gabus *et al.*, 2004) or by preventing an mRNA from going into the PB compartments. In fact, it is possible that mRNA silencing could be initiated in the diffuse cytoplasm before its final destination to PBs (Pillai *et al.*, 2005), and the prior binding of FMRP on such mRNAs could modulate their RISC susceptibility and thus affect the fate of the mRNAs. However, we could not see any impact on RISC activity of the presence of a G-quartet motif in the viscinity of miRNA targets, the main consensus motif known to be bound by FMRP (Schaeffer *et al.*, 2003). Thus, our data are in agreement with the proposal that FMRP is mostly associated with translated mRNAs (Corbin *et al.*, 1997) and whether these mRNAs should be submitted to silencing then they should dissociate from FMRP prior their final destination to PBs.

On the contrary, FMRP does not dissociate from the mRNAs submitted to a premature translation arrest (such as during cellular stresses) and accompany them into the SG storage compartments. Recruitment within SGs appears as a hallmark of the RNA-binding proteins. FMRP had been shown to follow this rule (Mazroui *et al.*, 2002). Furthermore, we showed that FMRP is likely to play a positive role in the SG formation. We evidenced here a defect in the stress granule formation process in absence of FMRP or in presence of a point mutation within its second KH motif, both causing the fragile X syndrome. Thus, FMRP adds to the list of RNA-binding proteins involved in SG formation after TIA-1, Pumilio2, and MLN51 (Gilks *et al.*, 2004; Vessey *et al.*, 2006; Baguet *et al.*, 2007). The exact contribution of SG proteins to SG formation during stress response appears unclear. SGs are consisting in stalled 48S preinitiation complexes proposed to participate to the reprogramming of mRNA metabolism for adaptation of cells to stress conditions (Anderson and Kedersha, 2006). In this process TIA-1 is proposed to play a structural role in the SG assembly process via the self-aggregation of its glutamine-rich motif in a prion-like manner (Gilks *et al.*, 2004). Meanwhile, these interactions are very dynamic as TIA-1 shuttles rapidly in and out the SGs (Kedersha *et al.*, 2000). Self-aggregation seems to be a characteristic of several of the SG proteins like G3BP (Tourriere *et al.*, 2003) and Pumilio2 (Vessey *et al.*, 2006). Whether FMRP has also some aggregation properties remains to be established. Alternatively, the defect in SG formation observed in the cells lacking FMRP could be due to the loss of an active role of FMRP in the process of translation inhibition. Our measurement of unaltered eIF2a phosphorylation levels in cells lacking FMRP upon stress (data not shown) do not favor this hypothesis however. Altogether our data provide strong lines of evidence for an involvement of FMRP in mRNA storage process during stress conditions. Also, because SGs and the neuronal RNA granules that are involved in the transport of silent mRNAs share many components (Anderson and Kedersha, 2006; Kiebler and Bassell, 2006), the defects reported for RNA granule formation in neurons lacking FMRP (Aschrafi *et al.*, 2005) could be related to the SG defects seen here. It will be important to determine now whether this defect in RNA granule formation is mostly affecting those mRNAs previously reported to be targeted by FMRP.

## ACKNOWLEDGMENTS

We thank T. Hobman (University of Alberta, Edmonton, Canada) for providing the anti-Ago2/Gerp95, J. Lykke-Andersen for anti-hDcp1a, C. Tomasetto (IGBMC, Illkirch, France) for anti-MLN51, and W. Filipowicz (FMI, Basel, Switzerland) for pEGFP-hAgo2. We are grateful to B. Bardoni, E. Khandjian, E. Bertrand for material and helpful discussions, S. Pannetier for care to Xfra mice, and M. Boeglin and P. Kessler for help with microscopy analyzes. MCD was supported by a PhD fellowship from the MinistèreDélégué à l'Enseignement Supérieur et à la Recherche and from Association pour la Recherche sur le Cancer. This project benefited from grants from National Institutes of Health (R01 HD40612-01), from Agence Nationale de la Recheche, and from the Fondation pour la Recherche Médicale and the Fondation Jerôme Lejeune to H.M.

## REFERENCES

Anderson, P., and Kedersha, N. (2002). Stressful initiations. J. Cell Sci. *115*, 3227–3234.

Anderson, P., and Kedersha, N. (2006). RNA granules. J. Cell Biol. *172*, 803–808.

Aschrafi, A., Cunningham, B. A., Edelman, G. M., and Vanderklish, P. W. (2005). The fragile X mental retardation protein and group I metabotropic glutamate receptors regulate levels of mRNA granules in brain. Proc. Natl. Acad. Sci. USA *102*, 2180–2185.

Baguet, A., Degot, S., Cougot, N., Bertrand, E., Chenard, M. P., Wendling, C., Kessler, P., Le Hir, H., Rio, M. C., and Tomasetto, C. (2007). The exon-junction-complex-component metastatic lymph node 51 functions in stress-granule assembly. J. Cell Sci. *120*, 2774–2784.

Barbee, S. A., *et al*. (2006). Staufen- and FMRP-containing neuronal RNPs are structurally and functionally related to somatic P bodies. Neuron *52*, 997–1009.

Bolte, S., and Cordelieres, F. P. (2006). A guided tour into subcellular colocalization analysis in light microscopy. J. Microsc. *224*, 213–232.

Castets, M., Schaeffer, C., Bechara, E., Schenck, A., Khandjian, E. W., Luche, S., Moine, H., Rabilloud, T., Mandel, J. L., and Bardoni, B. (2005). FMRP interferes with the Rac1 pathway and controls actin cytoskeleton dynamics in murine fibroblasts. Hum. Mol. Genet. *14*, 835–844.

Caudy, A. A., Myers, M., Hannon, G. J., and Hammond, S. M. (2002). Fragile X-related protein and VIG associate with the RNA interference machinery. Genes Dev. *16*, 2491–2496.

Cikaluk, D. E., Tahbaz, N., Hendricks, L. C., DiMattia, G. E., Hansen, D., Pilgrim, D., and Hobman, T. C. (1999). GERp95, a membrane-associated protein that belongs to a family of proteins involved in stem cell differentiation. Mol. Biol. Cell *10*, 3357–3372.

Corbin, F., Bouillon, M., Fortin, A., Morin, S., Rousseau, F., and Khandjian, E. W. (1997). The fragile X mental retardation protein is associated with poly(A)+ mRNA in actively translating polyribosomes. Hum. Mol. Genet. *6*, 1465–1472.

Cougot, N., Babajko, S., and Seraphin, B. (2004). Cytoplasmic foci are sites of mRNA decay in human cells. J. Cell Biol. *165*, 31–40.

Darnell, J. C., Jensen, K. B., Jin, P., Brown, V., Warren, S. T., and Darnell, R. B. (2001). Fragile X mental retardation protein targets G quartet mRNAs important for neuronal function. Cell *107*, 489–499.

Darnell, J. C., Mostovetsky, O., and Darnell, R. B. (2005). FMRP RNA targets: identification and validation. Genes Brain Behav *4*, 341–349.

De Boulle, K., Verkerk, A. J., Reyniers, E., Vits, L., Hendrickx, J., Van Roy, B., Van den Bos, F., de Graaff, E., Oostra, B. A., and Willems, P. J. (1993). A point mutation in the FMR-1 gene associated with fragile X mental retardation. Nat. Genet. *3*, 31–35.

Devys, D., Lutz, Y., Rouyer, N., Bellocq, J. P., and Mandel, J. L. (1993). The FMR-1 protein is cytoplasmic, most abundant in neurons and appears normal in carriers of a fragile X premutation. Nat. Genet. *4*, 335–340.

Dictenberg, J. B., Swanger, S. A., Antar, L. N., Singer, R. H., and Bassell, G. J. (2008). A direct role for FMRP in activity-dependent dendritic mRNA transport links filopodial-spine morphogenesis to fragile X syndrome. Dev. Cell *14*, 926–939.

Doench, J. G., Petersen, C. P., and Sharp, P. A. (2003). siRNAs can function as miRNAs. Genes Dev. *17*, 438–442.

Donze, O., and Picard, D. (2002). RNA interference in mammalian cells using siRNAs synthesized with T7 RNA polymerase. Nucleic Acids Res. *30*, e46.

Eulalio, A., Behm-Ansmant, I., Schweizer, D., and Izaurralde, E. (2007). P-body formation is a consequence, not the cause, of RNA-mediated gene silencing. Mol. Cell. Biol. *27*, 3970–3981.

Gabus, C., Mazroui, R., Tremblay, S., Khandjian, E. W., and Darlix, J. L. (2004). The fragile X mental retardation protein has nucleic acid chaperone properties. Nucleic Acids Res. *32*, 2129–2137.

Garber, K., Smith, K. T., Reines, D., and Warren, S. T. (2006). Transcription, translation and fragile X syndrome. Curr. Opin. Genet. Dev. *16*, 270–275.

Gilks, N., Kedersha, N., Ayodele, M., Shen, L., Stoecklin, G., Dember, L. M., and Anderson, P. (2004). Stress granule assembly is mediated by prion-like aggregation of TIA-1. Mol. Biol. Cell *15*, 5383–5398.

Huber, K. M. (2006). The fragile X-cerebellum connection. Trends Neurosci. *29*, 183–185.

Iacoangeli, A., Rozhdestvensky, T. S., Dolzhanskaya, N., Tournier, B., Schutt, J., Brosius, J., Denman, R. B., Khandjian, E. W., Kindler, S., and Tiedge, H. (2008). On BC1 RNA and the fragile X mental retardation protein. Proc. Natl. Acad. Sci. USA *105*, 734–739.

Ishizuka, A., Siomi, M. C., and Siomi, H. (2002). A Drosophila fragile X protein interacts with components of RNAi and ribosomal proteins. Genes Dev. *16*, 2497–2508.

Jin, P., Alisch, R. S., and Warren, S. T. (2004a). RNA and microRNAs in fragile X mental retardation. Nat. Cell Biol. *6*, 1048–1053.

Jin, P., Zarnescu, D. C., Ceman, S., Nakamoto, M., Mowrey, J., Jongens, T. A., Nelson, D. L., Moses, K., and Warren, S. T. (2004b). Biochemical and genetic interaction between the fragile X mental retardation protein and the microRNA pathway. Nat. Neurosci. *7*, 113–117.

Kawasaki, H., and Taira, K. (2003). Functional analysis of microRNAs during the retinoic acid-induced neuronal differentiation of human NT2 cells. Nucleic Acids Res. Suppl. *3*, 243–244.

Kedersha, N., Cho, M. R., Li, W., Yacono, P. W., Chen, S., Gilks, N., Golan, D. E., and Anderson, P. (2000). Dynamic shuttling of TIA-1 accompanies the recruitment of mRNA to mammalian stress granules. J. Cell Biol. *151*, 1257–1268.

Kedersha, N., Stoecklin, G., Ayodele, M., Yacono, P., Lykke-Andersen, J., Fritzler, M. J., Scheuner, D., Kaufman, R. J., Golan, D. E., and Anderson, P. (2005). Stress granules and processing bodies are dynamically linked sites of mRNP remodeling. J. Cell Biol. *169*, 871–884.

Kedersha, N. L., Gupta, M., Li, W., Miller, I., and Anderson, P. (1999). RNA-binding proteins TIA-1 and TIAR link the phosphorylation of eIF-2 alpha to the assembly of mammalian stress granules. J. Cell Biol. *147*, 1431–1442.

Khandjian, E. W., Huot, M. E., Tremblay, S., Davidovic, L., Mazroui, R., and Bardoni, B. (2004). Biochemical evidence for the association of fragile X mental retardation protein with brain polyribosomal ribonucleoparticles. Proc. Natl. Acad. Sci. USA *101*, 13357–13362.

Kiebler, M. A., and Bassell, G. J. (2006). Neuronal RNA granules: movers and makers. Neuron *51*, 685–690.

Laggerbauer, B., Ostareck, D., Keidel, E. M., Ostareck-Lederer, A., and Fischer, U. (2001). Evidence that fragile X mental retardation protein is a negative regulator of translation. Hum. Mol. Genet. *10*, 329–338.

Liu, J., Valencia-Sanchez, M. A., Hannon, G. J., and Parker, R. (2005). MicroRNA-dependent localization of targeted mRNAs to mammalian P-bodies. Nat. Cell Biol *7*, 719–723.

Mazroui, R., Huot, M. E., Tremblay, S., Filion, C., Labelle, Y., and Khandjian, E. W. (2002). Trapping of messenger RNA by Fragile X Mental Retardation protein into cytoplasmic granules induces translation repression. Hum. Mol. Genet. *11*, 3007–3017.

Nilsen, T. W. (2007). Mechanisms of microRNA-mediated gene regulation in animal cells. Trends Genet. *23*, 243–249.

Pillai, R. S., Bhattacharyya, S. N., Artus, C. G., Zoller, T., Cougot, N., Basyuk, E., Bertrand, E., and Filipowicz, W. (2005). Inhibition of translational initiation by Let-7 microRNA in human cells. Science *309*, 1573–1576.

Plante, I., Davidovic, L., Ouellet, D. L., Gobeil, L. A., Tremblay, S., Khandjian, E. W., and Provost, P. (2006). Dicer-derived microRNAs are utilized by the Fragile X Mental Retardation Protein for assembly on target RNAs. J. Biomed. Biotechnol. *4*, 1–12.

Rackham, O., and Brown, C. M. (2004). Visualization of RNA-protein interactions in living cells: FMRP and IMP1 interact on mRNAs. EMBO J. *23*, 3346–3355.

Schaeffer, C., Bardoni, B., Mandel, J. L., Ehresmann, B., Ehresmann, C., and Moine, H. (2001). The fragile X mental retardation protein binds specifically to its mRNA via a purine quartet motif. EMBO J. *20*, 4803–4813.

Schaeffer, C., Beaulande, M., Ehresmann, C., Ehresmann, B., and Moine, H. (2003). The RNA binding protein FMRP: new connections and missing links. Biol. Cell *95*, 221–228.

Sheth, U., and Parker, R. (2003). Decapping and decay of messenger RNA occur in cytoplasmic processing bodies. Science *300*, 805–808.

Sittler, A., Devys, D., Weber, C., and Mandel, J. L. (1996). Alternative splicing of exon 14 determines nuclear or cytoplasmic localisation of fmr1 protein isoforms. Hum. Mol. Genet. *5*, 95–102.

Stefani, G., Fraser, C. E., Darnell, J. C., and Darnell, R. B. (2004). Fragile X mental retardation protein is associated with translating polyribosomes in neuronal cells. J. Neurosci. *24*, 7272–7276.

Thermann, R., and Hentze, M. W. (2007). Drosophila miR2 induces pseudo-polysomes and inhibits translation initiation. Nature *447*, 875–878.

Tourriere, H., Chebli, K., Zekri, L., Courselaud, B., Blanchard, J. M., Bertrand, E., and Tazi, J. (2003). The RasGAP-associated endoribonuclease G3BP assembles stress granules. J. Cell Biol. *160*, 823–831.

Vessey, J. P., Vaccani, A., Xie, Y., Dahm, R., Karra, D., Kiebler, M. A., and Macchi, P. (2006). Dendritic localization of the translational repressor Pumilio 2 and its contribution to dendritic stress granules. J. Neurosci. *26*, 6496–6508.

Zalfa, F., Eleuteri, B., Dickson, K. S., Mercaldo, V., De Rubeis, S., di Penta, A., Tabolacci, E., Chiurazzi, P., Neri, G., Grant, S. G., and Bagni, C. (2007). A new function for the fragile X mental retardation protein in regulation of PSD-95 mRNA stability. Nat. Neurosci. *10*, 578–587.

Zalfa, F., Giorgi, M., Primerano, B., Moro, A., Di Penta, A., Reis, S., Oostra, B., and Bagni, C. (2003). The Fragile X syndrome protein FMRP associates with BC1 RNA and regulates the translation of specific mRNAs at synapses. Cell *112*, 317–327.

Zeng, Y., Yi, R., and Cullen, B. R. (2003). MicroRNAs and small interfering RNAs can inhibit mRNA expression by similar mechanisms. Proc. Natl. Acad. Sci. USA *100*, 9779–9784.

Zhang, Y. Q., Bailey, A. M., Matthies, H. J., Renden, R. B., Smith, M. A., Speese, S. D., Rubin, G. M., and Broadie, K. (2001). *Drosophila* fragile X-related gene regulates the MAP1B homolog Futsch to control synaptic structure and function. Cell *107*, 591–603.

Ziemiecki, A., Muller, R. G., Fu, X. C., Hynes, N. E., and Kozma, S. (1990). Oncogenic activation of the human trk proto-oncogene by recombination with the ribosomal large subunit protein L7a. EMBO J. *9*, 191–196.